



*Institute of Paper Science and Technology
Atlanta, Georgia*

IPST Technical Paper Series Number 673

Debris Characteristics and Removal Techniques

T. Bliss and M. Ostoja-Starzewski

August 1997

Submitted to
TAPPI 1997 Korea Recycling Symposium
Seoul, Korea
October 16–17, 1997

Copyright® 1997 by the Institute of Paper Science and Technology

For Members Only

INSTITUTE OF PAPER SCIENCE AND TECHNOLOGY PURPOSE AND MISSIONS

The Institute of Paper Science and Technology is a unique organization whose charitable, educational, and scientific purpose evolves from the singular relationship between the Institute and the pulp and paper industry which has existed since 1929. The purpose of the Institute is fulfilled through three missions, which are:

- to provide high quality students with a multidisciplinary graduate educational experience which is of the highest standard of excellence recognized by the national academic community and which enables them to perform to their maximum potential in a society with a technological base; and
- to sustain an international position of leadership in dynamic scientific research which is participated in by both students and faculty and which is focused on areas of significance to the pulp and paper industry; and
- to contribute to the economic and technical well-being of the nation through innovative educational, informational, and technical services.

ACCREDITATION

The Institute of Paper Science and Technology is accredited by the Commission on Colleges of the Southern Association of Colleges and Schools to award the Master of Science and Doctor of Philosophy degrees.

NOTICE AND DISCLAIMER

The Institute of Paper Science and Technology (IPST) has provided a high standard of professional service and has put forth its best efforts within the time and funds available for this project. The information and conclusions are advisory and are intended only for internal use by any company who may receive this report. Each company must decide for itself the best approach to solving any problems it may have and how, or whether, this reported information should be considered in its approach.

IPST does not recommend particular products, procedures, materials, or service. These are included only in the interest of completeness within a laboratory context and budgetary constraint. Actual products, procedures, materials, and services used may differ and are peculiar to the operations of each company.

In no event shall IPST or its employees and agents have any obligation or liability for damages including, but not limited to, consequential damages arising out of or in connection with any company's use of or inability to use the reported information. IPST provides no warranty or guaranty of results.

The Institute of Paper Science and Technology assures equal opportunity to all qualified persons without regard to race, color, religion, sex, national origin, age, disability, marital status, or Vietnam era veterans status in the admission to, participation in, treatment of, or employment in the programs and activities which the Institute operates.

DEBRIS CHARACTERISTICS AND REMOVAL TECHNIQUES

Terry Bliss,* Ph.D. Candidate
Dr. Martin Ostoja-Starzewski, Associate Professor
Institute of Paper Science and Technology
500 10th St. NW
Atlanta, GA 30318-5794 USA

*To whom correspondence should be addressed

ABSTRACT

The size, shape, density, stiffness, and surface chemistry characteristics of debris particles often control the effectiveness of debris removal with commonly used debris removal devices. The general trends which control debris removal for pressure screens, centrifugal cleaners, and suspended solids washing are reviewed. Some factors which limit the removal of marginally removable debris particles are discussed in greater detail.

Several stiffness and yield stress-based controlling mechanisms for the passage of easily deformable pressure sensitive adhesive particles (stickies) through fine slotted pressure screens are presented. Sticky particles with equivalent diameters up to four to five times larger than the nominal slot width are often accepted through the slots.

Recent reports show that removal of hot melt adhesive particles with centrifugal cleaners is difficult when the particle density is close to the density of water. A Bradley type debris removal efficiency model, and the expansion characteristics of polymeric adhesive components, are used to support a proposed mechanism to explain published results.

Debris particles smaller than 10 μm diameter can be readily removed via washing, but the chemistry conditions must be adjusted to suppress the natural surface attraction forces present. Particles larger than 1-5 μm are too large to be retained via surface attraction forces, especially under washing deinking chemistry conditions, but may be retained by mechanical filtration. Current research is correlating retention of suspended solids particles with fiber mat density (consistency), fiber coarseness, and fiber orientation bias within the mat.

INTRODUCTION

Two primary characteristics distinguish recovered fibers from never-dried virgin fibers: physical changes to the fibers themselves, and the presence of debris. The physical changes brought about by refining (especially cutting of fiber length, generation of fines, removal of the S1 layer of the fiber, and so on), and by drying (reduction in the potential to swell and conform within the sheet, addition of micro-compressions, etc.) are essentially the same whether the fibers are recycled internally and within the same grade (mill broke) or through commercial recovery of post consumer papers. Exceptions include the removal of dissolved and fine suspended solids via washing or similar techniques, the potential for treatment of fibers at elevated pH during deinking, and the tendency of post consumer recovered fibers to have a wide range of fiber species, kappa numbers, and refining histories. The variability characteristics are expected due to collection from a wide range of sources.

The presence of debris particles represents an extreme difference between post consumer recovered fibers and mill broke. Debris particles contribute to quality problems of all sorts: visual (specks, brightness), abrasion, clogging of equipment, deposits on machine clothing and other surfaces, picking, coating defects, and so on. It is not surprising that a major portion of most recovered fiber processing systems is devoted to debris removal.

A knowledge of debris characteristics is helpful for understanding the mechanisms of removal for various types of debris in commonly used unit operations. Classical debris removal mechanisms, and several newly proposed mechanisms are discussed.

DEBRIS CLASSIFICATION METHODS

It is convenient to classify debris according to size, shape, density, and surface characteristics, to help identify gross debris removal trends.

Size

Perhaps the best known system for generalizing the removal trends by major size dimension is that proposed by McCool and Silveri¹ in 1987, and reprinted by many other authors. A version is shown in Figure 1. This illustration suggests that commonly utilized progressive debris removal unit operations typically remove debris of about 0.5-1.0 order of magnitude size difference per step. It is important to note that the illustration is conceptual by nature; the unit operations overlap considerably, and no debris shape, density, or surface characteristics are taken into account.

Recent authors have argued that many unit operation efficiency curves should indicate essentially 100% removal efficiency above a certain size, rather than a peak efficiency at a particular debris particle size.²

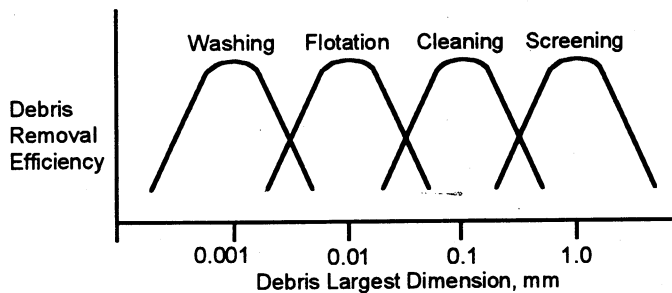


Figure 1: Conceptual debris removal efficiency vs. size curve for various unit operations (adapted from McCool and Silveri¹).

Shape

The above discussion assumes that the particle's major dimension is dominant for removal in most unit operations. Strong theoretical and experimental evidence shows that particle shape profoundly affects debris removal efficiency for most unit operations. A debris shape classification protocol described by Bliss³ lists the number of long dimensions:

- 0 long dimensions is small cubical debris.
- 1 long dimension is long or splinter-like debris;
- 2 long dimensions is flat or flake-like debris;
- 3 long dimensions is large cubical debris;

In the context of the original reference, the term *long* is relative to pressure screen hole diameter or slot width, and assumed to be several times longer than the other dimensions. Typical particles classified by this system are shown in Figure 2.

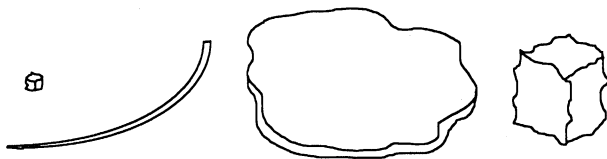


Figure 2: Debris particles with 0, 1, 2, and 3 long dimensions.

It is clear that particle orientation is relevant only for debris with 1 or 2 long dimensions. Such particles are oriented primarily by fluid flow within process equipment. In

general, drag on the surface of a particle tends to keep the particle within a stream flow line, and oriented with its longest dimension parallel to the direction of travel, while fluid-particle density differential tends to encourage the particle to cross fluid streamlines as their direction changes. The effect of particle shape must be evaluated based on a knowledge of the mechanism of debris particle removal within a particular unit operation.

Density

Particle density, or, more properly, the difference in density between the particle and the suspending fluid, is the driving force for particle separation efficiency in centrifugal cleaners. However, particle density also influences the particle drag to mass ratio, which means there is an interaction between the effects of size, shape, and density difference. All of these variables significantly affect debris removal efficiency in centrifugal cleaners; consideration of only one will at best predict results for limited conditions.

Surface Characteristics

Particle surface characteristics cover a variety of properties, including cohesion/adhesion properties, and wetting characteristics. Debris particles may agglomerate, become coated with other materials, or deposit on surfaces. Agglomeration may change the shape or size of particles, while attraction of other substances may contribute to agglomeration, passivation, or changes in the density of the agglomerated particle.

ADHESIVES: A SPECIAL PROBLEM FOR RECOVERED PAPER

Adhesives in general represent a particularly troublesome category of debris for recovered paper. While many other classes of debris are present in larger quantities, adhesives as a class, and especially formulations which are extremely soft, tacky, and close to 1.0 g/cm³ in density, are problematic and difficult to remove. The problems caused by adhesives include visual defects in the finished sheet; deposits in fabrics, and on dryers, rolls, and many other surfaces; reduction in slide angle; and picking. These problems are well documented in the literature; examples are found in references 4-6.

Doshi⁷ has classified sticky adhesives into three categories: hot melt adhesives, pressure-sensitive adhesives, and lattices.

Hot melt adhesives (HMA) are used for book binding, sealing corrugated cartons, and occasionally as a moisture barrier. They are relatively soft solids at room temperature, but are applied as viscous liquids at temperatures above their

softening temperature (150-250 °C), and form bonds as they cool. The most common formulation for hot melt adhesives is based on ethylene vinyl acetate (EVA) copolymers, with tackifiers added. While EVA is generally insoluble in water, acids, or alkali, some added components can leach out in water, and the adhesive itself is soluble in some organic solvents. HMA density can range from 0.89 to 1.3 g/cm³.

Hot melt adhesives cause mostly appearance problems. Larger particles are removed by pressure screens, and smaller particles are removed primarily by forward or reverse/through flow cleaners, depending on their density.⁸⁻⁹ HMA particles smaller than 200 µm can be removed with modest efficiency via froth flotation,^{10,11} and particles smaller than about 10-20 microns can be removed with reasonable efficiency via washing.¹² In addition, hot dispersion can be used to reduce HMA particle size from visible to non-visible.¹³

Pressure sensitive adhesives (PSA) are used for tapes, labels, and self-seal envelopes. They usually consist of an elastomeric polymer such as natural rubber, styrene-butadiene rubber (SBR), polyisoprene rubber, copolymers of styrene and isoprene, polyacrylates, and vinyl acetate/acrylate copolymers. Tackifiers, plasticizers, fillers, viscosity modifiers, and stabilizers are often mixed with these polymers to modify their properties.^{7,14,15}

Adhesive properties tend to be specific to the blend, and can be profoundly different even for a stereoisomer of the same compound. For example, Hsu¹⁶ points out that at 50 °C, natural rubber (cis-1,4-polyisoprene) is tacky, while its stereoisomer, (trans-1,4-polyisoprene) is crystalline and hard. PSAs are generally tacky at room temperature, and usually have a T_g (glass transition temperature) well below room temperature. While most PSA materials are insoluble under neutral aqueous conditions, polymers containing carboxyl groups, including acrylics, casein, and shellac, are often soluble under alkaline conditions, and form macro size agglomerates when an alkaline pulp suspension is acidified. The latter, commonly called "acid shock" in deinking, is a potential source of agglomerated sticky particles and deposits. Leaching of components from adhesives, absorption of trace components from the paper slurry (especially oils), attachment of or to other particles, or exposure to light or bleaching chemicals, could also result in changes in PSA mechanical properties, such as tack, density, surface characteristics, stiffness, particle size and shape.

Pressure sensitive adhesives cause appearance problems, a variety of deposit and fabric filling problems, and picking during papermaking and printing. They are repeatedly identified as the most significant quality complaint for users

of recovered fiber, and are especially problematic when deinked fiber is used for fine paper applications. Larger particles are removed with fine slotted pressure screens, and smaller particles are removed with forward or reverse/through flow cleaners, depending on their density. As with HMA, PSA particles smaller than 200 µm can be removed with modest efficiency via froth flotation,^{10,11} and particles smaller than 10-20 µm can be removed via washing.

Lattices consist of particles of rubber dispersed in water. Protective colloids and other stabilizing agents keep the rubber particles dispersed and prevent agglomeration or coagulation. Many of the same elastomeric compounds that are used in PSA formulations are also available in latex form, and can be used for coatings, and for heat seal applications. They are characteristically similar to PSA.

REMOVAL TECHNIQUES

Common unit operations used to remove adhesive particles from paper fiber slurries include pressure screens, centrifugal cleaners, washers, and froth flotation. The efficiency of these unit operations for removal of adhesive particles will be discussed with respect to particle size, shape, stiffness, yield stress, and other physical or mechanical properties. While the general trends are well known, new mechanisms for adhesive particle removal are proposed and evaluated using data from the literature.

Pressure Screens

Pressure screens have been used to remove debris from paper stock since 1939.³ A pressure screen typically consists of a screen plate with restrictive holes or slots; a rotor, which imparts a periodic backflushing pulse to clear mats of fiber and debris particles from the inlet side of the screen plate; and separate discharge paths for accepted and rejected stock.

During operation, pressure from the feed pump forces stock through the small holes or slots in the screen plate. But, since the hole diameter or slot width is much smaller than the fiber length or some debris particle dimensions, water passes through the holes or slots more readily than fibers or debris particles, and the holes or slots tend to become blocked with a mat of fibers and debris particles. A pulsation producing element mounted on a rotor produces a periodic backflushing pulse which removes the matted material, draws some previously accepted stock or water back through the plate, and re-mixes the material on the feed side of the plate, as often as 50 times per second. The rotor

pulsation pattern can have a variety of shapes, as shown by Yu,¹⁷ depending on the rotor design.

Figure 3 shows examples of screen plates with slots and holes, and various shapes of debris particles. It is clear that debris orientation is critical for the rejection of 1-long and 2-long dimension particles. The fluid motion imparted by the rotating element tends to align the long dimensions of these debris particles with the direction of rotation, thus providing an orientation favorable for rejection for particles which are stiff enough to resist being deformed through the holes or slots.

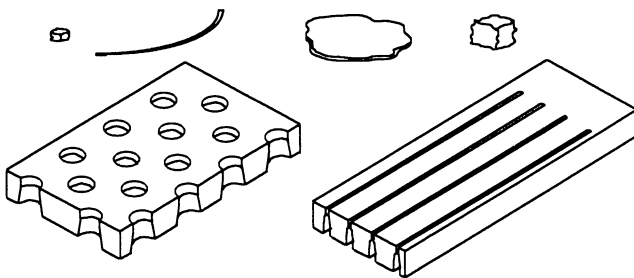


Figure 3: Screen plates with holes (left) and slots (right); debris particles of various shapes.

For the last 20 years screen plates with surface contours on their inlet surface have also been available. If a screen plate has a contour on its inlet surface, and the rotating element is also on its inlet surface, the fluid flow patterns near the screen plate openings are disrupted (localized “micro-turbulence” is created), which tends to reduce the extent of debris and fiber alignment. This increases the capacity of the screen, reduces its tendency to preferentially reject longer, coarser fibers, and allows operation at lower reject rates; hence, the capital and operating costs of the installation are reduced. However, debris removal efficiency is also reduced, necessitating smaller hole diameter or slot width to provide the same debris removal efficiency.³

Factors affecting debris removal efficiency

A large number of factors have been found to affect debris removal efficiency in pressure screens. These factors can be conveniently divided into design variables, and operating variables.³

Design variables include:

- Rotor design;
- Rotor speed (slower is generally better);
- Flow path through the screen (rotor on the inlet side allows debris alignment on the inlet side);
- Holes vs. slots (slots are better for 0-long particles);
- Hole diameter or slot width (smaller is better);

- Slot orientation (slot length perpendicular to rotation is better);
- Screen plate surface contour (a more aggressive contour reduces debris removal efficiency);

Operating variables include:

- Feed consistency (higher is better);
- Reject rate (higher is better);
- Pressure drop, measured from inlet to accept (lower is better);
- Temperature (lower is better).

Mechanisms of debris removal

Many mechanisms have been presented for debris removal in pressure screens; however, the two most often cited in the literature, and best supported by experimental data, are positive size separation, and debris alignment.

Positive size separation depends on all of the debris particle dimensions being larger than the hole diameter or the slot width, on the assumption that all particles are presented with the opportunity to pass through a hole or slot thousands of times between their initial approach to the screen plate, and their departure from the screen in the reject stream. Positive size separation is not practical for removal of all debris of interest, because slot widths of 100-150 μm are required to allow reasonable throughput rates at practical consistencies. Unfortunately, 100-150 μm is well within the range of visibility to the unaided eye. Particles of this size range are often considered to be visually objectionable, and could also potentially cause picking, deposits, and streaks in blade coated paper.

Debris alignment results from the tendency of 1-long and 2-long dimension debris particles to align their longest dimension with the direction of rotation. Thus, splinter-like debris particles are presented to holes with their length facing the holes, and to slots with their length perpendicular to the slot width, while flake-like debris particles are presented to holes and slots with their flat surfaces parallel to the screen plate surface. This allows debris particles which could easily pass through the holes or slots to be rejected because they are oriented for rejection.

Unfortunately, orientation also tends to discourage fiber passage, especially at higher feed consistencies, unless the fibers are sufficiently flexible to be passed by bending. Passage of fibers by bending through the slots has been reported by Yu and DeFoe¹⁸ based on magnified visual observation in a simulator. This mechanism probably passes fibers less efficiently than the straight through passage mechanism reported by others,¹⁹ especially at normal

operating consistencies, where fiber entanglement is significant.

In recent years, the trend has been toward the use of more aggressive screen plate inlet surface contours, to allow the use of smaller diameter holes, and narrower slots. This has resulted in a trend away from debris alignment, and toward positive size separation, as the controlling mechanism.

Several novel debris removal mechanisms are presented here for relatively soft, easily deformable adhesive particles, based on data and observations from the literature. A number of literature sources²⁰⁻²² and anecdotal reports from numerous mills indicate that sticky adhesive particles much larger in equivalent diameter than the nominal slot width sometimes appear to be removed with very low efficiency. For example, Figure 4 shows removal efficiency vs. equivalent diameter for pressure sensitive adhesives (repulped self-stick address labels) with a pressure screen fitted with a cylinder containing 150 μm nominal width slots and a mild surface contour, for various calculated nominal velocities through the slot. Details of the experimental procedure can be found in references 20 and 21. At low feed consistency (1.25%, in this case), calculated nominal velocity is essentially linearly proportional to pressure drop across the screen plate. The debris removal efficiency is only 25-30% for PSA debris particles with equivalent diameters of 450- 600 μm , up to 4-5 times the nominal slot width. When the equivalent diameter increases to 600-750 μm , there is a sudden increase to 60-70% removal efficiency.

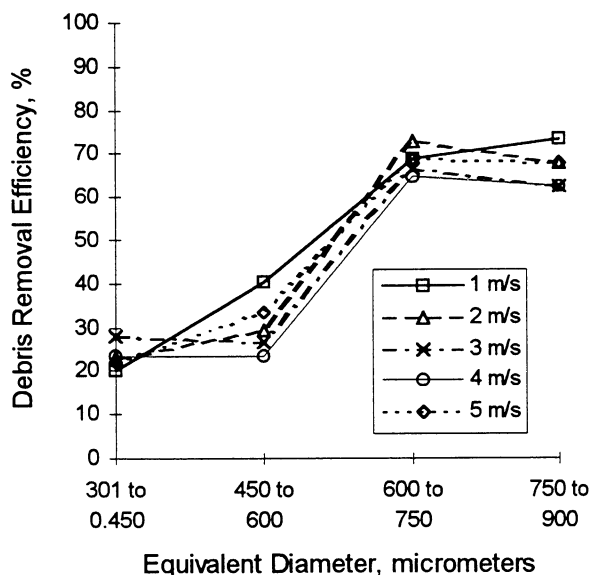


Figure 4: PSA particle removal efficiency vs. particle equivalent diameter, for 150 μm width slots, at various nominal velocities through the slot.²⁰

The apparent contradiction in debris particle size passed vs. nominal slot size can now be explained by any of the following proposed mechanisms of debris removal: particle shape ratio and alignment; bending resistance of beams; and, extrusion of low yield stress particles.

Particle shape ratio and alignment is based on the shape ratio of the debris particles in their three axes (major, middle, and minor), and the assumption that inlet surface contour patterns commonly used for pressure screen cylinders today impart sufficient turbulence to allow most of the debris particles to approach at least one slot with their smallest dimensions parallel to the slot width (i.e. oriented for passage through the slot). These conditions are more likely to occur for particles with shape ratios that are not too extreme, such that alignment with the flow streamlines is less likely.

Adhesive layer thickness for the original application can range from 25-50 μm for PSA tapes, to 1 mm for HMA used for sealing cartons.¹⁴ During processing, the adhesive particles can undergo size reduction, due to impacts or shear; agglomeration, due to impact of particles which have an affinity for each other; or, shape changing, due to self-adhesion (i.e. the particle rolls or folds onto itself). In a high shear environment, particles are subject to impacts of near-random intensity and orientation. This should result in chipping along the edges, and fracture along the particle's shortest dimension. The latter is because the force necessary to break the particle in its shortest dimension is lower, and the probability of impact parallel to the shortest dimension is higher than the probability of impact parallel to the longer dimensions.

For homogeneous, isotropic materials, particles should tend to become more spherical as they fracture many times. This near spherical shape could be described as having a major:middle:minor axis ratio of about 1:1:1, as a limit. But, when a nearly spherical particle fractures (other than a minor chip), it forms two particles with shape ratios of 2:2:1; the next time it fractures, the fragments probably have shape ratios of 2:1:1; and, after one more fracture, about 1:1:1.

In reality, fractures may occur in less likely places as well, thus contributing to a somewhat wider shape ratio distribution than suggested above. Experimental data describing the characteristic three dimensional shape of adhesive particles is unfortunately not readily available in the literature. For the purpose of the calculations which follow, a potato-shaped particle is assumed, with a 4:2:1 shape ratio.

The equivalent diameter data on the x axis of Figure 4 was obtained via image analysis, which is the normal method for quantification of debris particle size today. However, if the particle has a shape other than spherical, most image analysis sample preparation techniques will result in the two largest dimensions being presented to the camera or scanner. This can result in a significant over-estimation of the equivalent spherical diameter, which, when combined with the potato shape and 4:2:1 shape ratio discussed above, can account for the debris particle removal data shown in Figure 4. This can be seen by recalling that the area for an ellipse is calculated as shown in Equation 1:

$$Area = \pi ab/4 \quad (Equation 1)$$

where a and b are the lengths of the major and minor axes, respectively. If the equivalent diameter is expressed as projected area, the length of the major and minor axes can be calculated for the condition $a = 2b$. Then, assuming that the minor axis from this projected view is actually the middle axis of the three dimensional particle, and that the middle axis may be twice the true minor axis, the dimensions of a potato-shaped particle of 4:2:1 shape ratio are calculated. Particle dimensions calculated by this method of analysis are compared to particle size as measured by image analysis in Table 1, for the largest particle size range which shows low removal efficiency, and the smallest particle size range which shows high removal efficiency, from Figure 4.

Table 1: Measured vs. calculated dimensions of PSA particles. Image analysis calibration = 39 $\mu\text{m}/\text{pixel}$.

| Measured particles (via image analysis) | | Calculated (potato-shaped) particle axes dimensions (μm) | | |
|---|------------------------|---|-------------|------------|
| Equivalent dia. (μm) | Area (mm^2) | Major axis | Middle axis | Minor axis |
| 450-600 | 0.159-0.283 | 636-848 | 318-424 | 159-212 |
| 600-750 | 0.283-0.442 | 848-1060 | 424-530 | 212-265 |

The two values in each cell of the first two columns of Table 1 are the minimum and maximum values for the original image analysis data bins. The two values in each cell of the last three columns correspond to the minimum and maximum axis length calculated for a “potato-shaped” particle having a projected area equivalent to that of the measured particles. Tolerance requirements for machined slots in screen plates usually require that approximately 90% of the slot widths are within 50 μm of the nominal slot size. Thus, the nominal 150 μm slotted screen cylinder used for the trial which generated the data shown in Figure 4 and Table 1 contained mostly 100-200 μm width slots. If most of

the particles are eventually presented with their smallest dimension parallel to the width of a 200 μm width slot, most of the 450-600 μm equivalent diameter debris particles should eventually be accepted, while most of the 600-750 μm equivalent diameter particles should be rejected. Thus, a sharp debris removal efficiency transition over the indicated range, as seen in Figure 4, is explained.

The next three mechanisms described are all based on resistance of the debris particle to mechanical deflection, and all assume that the debris particle bridges across the slot. Debris particle deformation as a mechanism controlling particle passage has been proposed in the literature a number of times,²⁰⁻²³ but no theoretical or conclusive experimental data has been presented to confirm its occurrence.

A simple, first order evaluation of the potential for debris particles to deflect can be performed by modeling deflection of a simple supported beam, with an applied load consisting of the particle area multiplied by the pressure drop across the screen plate. It is assumed that the particle is isotropic and homogeneous, and that the deflection is very small, such that the maximum angle of deflection is < 0.1415 radians (the model requires that the cosine of the maximum angle of deflection $\cong 1$) in order to ensure that the material is still within its linear elastic range, where Hooke’s Law is valid. In view of these restrictions, this analysis could be considered only as a lower limit case, meaning that if the material is too stiff to deflect to this extent, bending deflection probably is not responsible for passage of the particle. Figure 5 shows the beam deflection setup as a free body diagram. The maximum deflection and the maximum angle of deflection are calculated according to Equations 2 and 3, respectively:²⁴

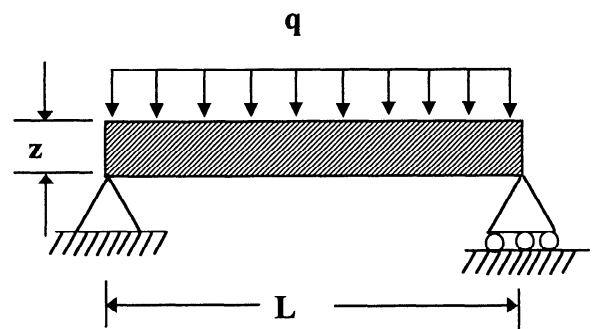


Figure 5: Free body diagram for beam deflection analysis.

$$Maximum Deflection = \delta_{max} = \frac{5qL^4}{384EI} = \frac{60dpL^4}{384Ez^3} \quad (Equation 2)$$

$$\text{Maximum Angle of Deflection} = \theta_{\max} = \frac{qL^3}{24EI} = \frac{dpL^3}{2Ez^3}$$

(Equation 3)

where q = force per unit length, E = modulus of elasticity (Young's modulus), I = moment of inertia = $bz^3/12$, b = particle width (perpendicular to the plane of the page), and dp = pressure drop = q/b .

The Young's modulus values of some common adhesive components, and other polymers, are listed in Table 2.

Table 2: Young's modulus and yield stress values for selected polymers utilized in adhesive formulations.^{15,24-26}

| Polymer | Young's Modulus (MPa) | Yield Stress (MPa) |
|------------------------------------|-----------------------|--------------------|
| Polyethylene | 100-600 | 8-35 |
| Polypropylene | 10 | 35 |
| Polystyrene | 2700-4100 | |
| Polyvinylchloride | 1400-4100 | |
| Rubber | 0.7-4.0 | 1-7 |
| Commercial acrylic PSA | 0.05-0.3 | |
| SIS or SBS rubber block copolymers | | 0.5 |

The values listed in Table 2 clearly show that the Young's modulus values for the elastomeric materials typically used in PSA formulations are 3-5 orders of magnitude lower than those of the engineering plastics, which could be used for tape backings, packaging film, bags, wrap, or hot melt adhesives. This is because PSAs must be flexible enough to wet an adherend surface at the application temperature with very little applied load, which means that they must be much more conformable than engineering plastics. This fact is emphasized by the general difficulty in obtaining good modulus data in the literature for rubbery materials; most elastomeric materials are characterized by modulus data at 100-700% extension, which is not appropriate for this analysis. The shear strength of the bonds formed by PSA materials are also several orders of magnitude below that of other adhesives, as shown in Table 3.²⁷

Table 3: Shear load capabilities of adhesives.

| Adhesive Type | Shear Load (MPa) |
|--------------------|------------------|
| Pressure sensitive | 0.005-0.02 |
| Rubber based | 0.3-7 |
| Emulsion | 10-14 |
| Hot melt | 1-15 |
| Polyurethane | 6-17 |
| Epoxy | 14-50 |

For the beam deflection analysis, nominal pressure drop across the screen plate is taken as 15-70 kPa, and, $L = 150 \mu\text{m}$, the nominal slot width. Values of 0.1 and 1000 MPa are assumed for E . The resulting values for δ_{\max} and θ_{\max} are listed in Table 4, for particles which are thinner than half the nominal slot width, since thicker particles could not fit through the slot when folded in half.

Table 4: Maximum deflection and maximum angle of deflection for particles bridging a 150 μm slot under a pressure drop of 15 and 70 kPa.

| Young's modulus = 0.1 MPa (typical PSA) | | | | |
|--|---|--------|--------------------------------------|--------|
| | Pressure drop | | Pressure drop | |
| | 15 kPa | 70 kPa | 15 kPa | 70 kPa |
| Particle thickness (μm) | Max deflection, δ_{\max} (μm) | | Max angle, θ_{\max} (radians) | |
| 75 | 28 | 131 | 0.6 | 2.8 |
| 50 | 95 | 443 | 2.02 | 9.45 |
| Young's modulus = 1000 MPa (typical engineering plastic) | | | | |
| | Pressure drop | | Pressure drop | |
| | 15 kPa | 70 kPa | 15 kPa | 70 kPa |
| Particle thickness (μm) | Max deflection, δ_{\max} (μm) | | Max angle, θ_{\max} (radians) | |
| 75 | 0.003 | 0.013 | <0.0001 | 0.0003 |
| 50 | 0.010 | 0.044 | 0.0002 | 0.0009 |
| 25 | 0.076 | 0.354 | 0.0016 | 0.0075 |
| 15 | 0.352 | 1.640 | 0.0075 | 0.0350 |
| 5 | 9.500 | 44.29 | 0.2025 | 0.9450 |

It is clear from the data in Table 4 that deflection can be quite significant for thin particles, and for very low modulus particles, in fact beyond the model limit of $\theta_{\max} = 0.1415$ radians, when the particle thickness is below 75 μm for PSA particles, or below 5-10 μm for engineering plastics. This indicates that significant bending deflection cannot be ruled out for low modulus PSA particles which are thinner than half the slot width.

This analysis suggests but does not prove that massive bending deflection may occur, since the assumptions of the beam deflection model are too restrictive to allow for evaluation of that case.

A perfectly-plastic hinge bending model is much better suited for very large distortions under load than a simple beam bending model. Figure 6 shows an idealized stress-strain diagram for an elastic-perfectly plastic material. The initial high slope zone is the elastic deformation zone, where Hooke's Law applies, and defines the limit of the previous beam deflection example, which is limited to very small deformations. After the yield stress σ_y is reached, the material deforms perfectly plastically, meaning that it deforms at constant stress.

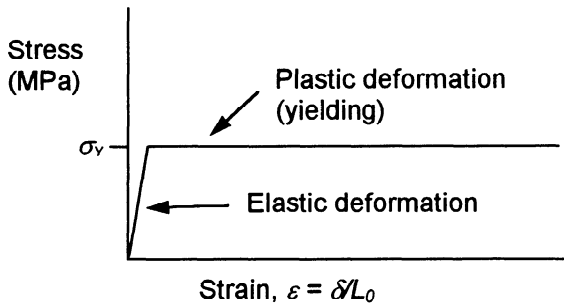


Figure 6: Stress-strain diagram for an elastic-perfectly plastic material.

If a beam as shown in Figure 5 is loaded above the elastic limit, or yield stress, σ_y , the maximum bending moment at yield, M_y , is reached. This relationship is summarized in Equation 4:

$$q > q_y = \frac{8M_y}{L^2} \quad (\text{Equation 4})^{24}$$

M_y for a rectangular cross section beam is described by Equation 5:

$$M_y = \frac{\sigma_y b z^2}{6} \quad (\text{Equation 5})^{24}$$

Substituting Equation 5 into Equation 4, and using the relationship $dp = q/b$, Equation 4 can be rewritten as Equation 6 to determine dp_y = the pressure drop at which the yield stress is exceeded:

$$dp_y = \frac{8\sigma_y z^2}{6L^2} \quad (\text{Equation 6})$$

As the load increases beyond this level, a so-called plastic hinge develops at the midpoint. This occurs at $M = M_p = 1.5M_y$ and at load $q_p = 1.5q_y$. Equation 6 can then be rewritten as Equation 7:

$$dp_p = \frac{3}{2} \left[\frac{8\sigma_y z^2}{6L^2} \right] = \frac{2\sigma_p z^2}{L^2} \quad (\text{Equation 7})$$

The feasibility of the perfectly-plastic hinge bending model is evaluated for values of $\sigma_y = 0.1, 1.0,$ and 10 MPa, covering the range of elastomeric and engineering polymer yield stress values listed in Table 2. The calculated values for the pressure drop necessary to cause plastic hinge bending are listed in Table 5.

Table 5: Pressure drop necessary to cause plastic hinge bending of debris particles through a 150 μm wide slot.

| Yield stress (MPa) | Particle thickness (μm) | Pressure drop (kPa) |
|--------------------|--------------------------------------|---------------------|
| 0.1 | 50 | 22.2 |
| 0.1 | 75 | 50 |
| 1.0 | 5 | 2.2 |
| 1.0 | 15 | 20 |
| 1.0 | 25 | 55 |
| 1.0 | 50 | 222 |
| 10 | 5 | 22.2 |
| 10 | 15 | 200 |

The pressure drop values in Table 5 are below $dp = 70$ kPa for virtually any particle thickness below $75 \mu\text{m}$ for the yield stress values typical of pressure sensitive adhesives, indicating the feasibility of this mechanism for passage through the slot. By comparison, the engineering plastics probably have high enough yield stress values to resist passage through the slots by the plastic hinge mechanism except when they are very thin, perhaps under $10 \mu\text{m}$.

The bending models have been evaluated only for relatively thin particles, since the particle thickness must be less than half the slot width in order to pass through the slot in a folded condition. Theoretically, particles of virtually any thickness could pass through a slot by an extrusion mechanism. An extrusion model can be constructed from a model originally intended for drawing wires in a die. Such an ideal (frictionless) die would have a tapered inlet side, with yielding material on the inlet side, which is under a load, as shown in Figure 7. In this case, A_1 is the cross sectional area of the tapered inlet side at its maximum diameter; A_2 is the cross sectional area of the discharge side

at the minimum diameter point; P_1 is the force applied against the inlet side, and P_2 is the force pulling the material from the discharge side. D_1 and D_2 represent the diameters of the inlet taper and the minimum diameter, respectively, as shown in Figure 7.

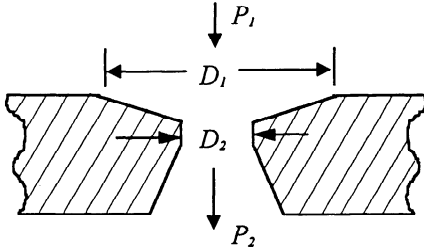


Figure 7: Geometry for the extrusion model

The relationship between the various forces and geometric parameters is given by Equation 8:

$$\frac{P_1}{A_1} + \frac{P_2}{A_2} = 2\sigma_Y \ln \frac{D_1}{D_2} \quad (\text{Equation 8})^{28}$$

For the example where the cross section shown in Figure 7 is the cross section of a commercial 1.3 mm nominal diameter hole in a screen plate with a contoured inlet surface, as shown in Reference 3, P_1/A_1 can be interpreted as the force per unit area (pressure) on the inlet side of the screen plate, and likewise the term P_2/A_2 is the accept pressure. Since the accept pressure tends to resist the passage of the material, it is subtracted, to yield dp , pressure drop, on the left hand side. Taking values of 4.5 and 1.3 mm for D_1 and D_2 , respectively, and solving for σ_Y shows that at normal pressure drops, the particle's yield stress must be below 0.01 to 0.03 MPa for extrusion to occur. Extrusion seems unlikely to occur, given the range of yield stress values listed in Table 2.

The extrusion model suggests that the pressure drop necessary to extrude material is independent of the nominal hole diameter, due to the frictionless assumption. The frictionless assumption also explains why the model tends toward zero pressure drop as the taper on the inlet side reduces to a non-tapered hole (i.e., when $D_1 = D_2$, such that $\ln(D_1/D_2) = 0$), meaning that no pressure drop is consumed, and no extrusion takes place, as a plug of material passes through a non-tapered cylinder. These assumptions are generally reasonable for drawing metals through a die, since the friction effect would be very small relative to the high yield stress of metals. However, when the yield stress is very low, and when the hole diameter or slot width is very small, the frictional resistance effect may be quite significant relative to the yield stress. Also, as D_1 is reduced, friction is

reduced proportional to D_1 , while total applied force on the inlet side (P_1) is reduced proportional to $0.5D_1^2$, given similar geometry in the taper. This suggests that significant additional pressure drop would be required to extrude a particle, or, for a fixed pressure drop, that extrusion will not occur unless the yield stress is even lower than the 0.01-0.03 MPa range previously determined, for the case of extrusion of adhesive materials through very small holes or slots.

The extrusion model is also independent of particle thickness, which means that in theory, a particle of virtually any size can be extruded through any hole size, if the pressure drop is higher than the minimum required per Equation 8. This suggests that if extrusion were occurring, the sharp increase in removal efficiency at a particular equivalent diameter, as noted in Figure 4, should not occur.

In summary, the shape ratio and alignment model completely explains the debris removal efficiency trends shown in Figure 4 independently of particle strength properties. Both of the bending models suggest that folding is a viable mechanism for passage of PSA particles less than 75 μm thick, and perhaps for some plastic film particles less than 10 μm thick. Toner particles, in the absence of agglomeration or self-adhesion, certainly fit in the latter category. Lacking a knowledge of the PSA particle thickness distribution for the case illustrated, it is not possible to distinguish whether shape ratio and alignment, or bending, is responsible for the behavior observed in Figure 4.

The extrusion model seems less likely, due to its limitation to extremely low yield stress materials for normal screen pressure drops, and since its predicted behavior characteristics do not seem to be consistent with the debris removal efficiency trends shown in Figure 4.

The most likely models all suggest that the use of the smallest possible nominal slot width makes sense, for improved debris removal efficiency. Preserving the debris particle size, or agglomerating to a larger size could also be helpful.

It is also possible that some chemical treatment to improve the Young's modulus or yield stress may be feasible. In recent articles, Naddeo and coworkers²⁹⁻³¹ have proposed detackification of pressure sensitive adhesives with an oxygen delignification treatment, and Hsu¹⁶ has suggested that oxygen or other bleaching treatments may increase particle stiffness and hence improve particle removal during screening. Stiffness is related to the degree of cross-linking of the polymer chains, which can be enhanced by oxidizing unsaturated double bonds, in SBR based adhesives. But, oxidation will cleave the polymer chains of SIR based

adhesives, which may reduce stiffness. Oxidation will probably have minimal effect on acrylic based adhesives, since they have no unsaturated bonds.¹⁵

Centrifugal Cleaners

Centrifugal cleaners have been used industrially for nearly 100 years to remove sand, and other dense materials from paper fiber slurries. A classical centrifugal cleaner consists of a conical or cylindrical-conical pressure vessel with a tangential inlet, and coaxial outlets on the base of the cone (the overflow) and at the apex of the cone (the underflow). They are widely used in the paper industry today, in sizes ranging from 100 cm to as small as 7.5 cm primary diameter.³² This discussion addresses the characteristics and applications of smaller diameter, continuous rejecting fine cleaners.

During operation, stock is fed under pressure into the inlet, where its tangential orientation initiates a swirling pattern within the cleaner. The slurry follows a well ordered flow pattern down the inside diameter of the cleaner, which means the tangential velocity must increase as the cross sectional area of the cone decreases. High velocity in an ever-changing direction causes materials more dense than the suspending fluid (sand, grit, ink balls, bark particles, etc.) to migrate through the fluid streamlines, toward the inside wall of the cone. Likewise, particles less dense than the suspending fluid (certain adhesives, wax, polystyrene foam, and air bubbles) tend to cross fluid streamlines as they migrate toward the central axis of the cleaner. As the fluid flow approaches the apex (underflow) outlet, only a fraction of the fluid can exit out the apex opening, due to the restrictive size of the opening. Most of the flow reverses its axial direction, and follows a smaller diameter spiral path up the interior of the cleaner, where it exits out the coaxial outlet in the base of the cone.

Cleaners used to remove high density debris are usually called forward cleaners today, to distinguish them from the more recent application of low density debris removal, usually called reverse cleaning. Forward cleaners usually discharge a very small fraction of the fluid and solids from a very small apex opening, called the rejects outlet in that application. Reverse cleaners use much larger openings at the apex end, and discharge a much larger fraction of the fluid, and most of the solids, from the apex end. The underflow opening is the exit point for accepted stock from a reverse cleaner. Figure 8 illustrates these two applications of small diameter centrifugal cleaners, and shows typical flow splits and consistencies.

Also included in Figure 8 is a third type of centrifugal cleaner, popularly called a through flow cleaner, which discharges both its accepts (the outer-most stream) and its rejects (the inner-most stream) from the apex end of the cleaner. Since through flow cleaners remove low density debris particles in their reject streams, they are functionally competitive with reverse cleaners.

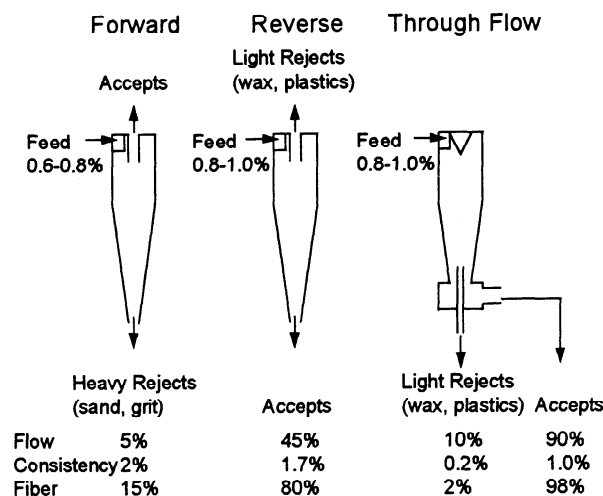


Figure 8: Forward, reverse, and through flow cleaners.

The design and operating trends which affect centrifugal cleaner debris removal efficiency are generally well known:

Design variables:

- Primary diameter (smaller is better);
- Cleaner length (longer is better);
- Cone angle (smaller is better);
- Inlet area (smaller is better);
- Surface characteristics (hydraulically smooth is better);

Operating variables:

- Pressure drop (higher is better);
- Feed consistency (lower is better);
- Reject rate (higher is better);
- Temperature (higher is better).

As with pressure screens, manipulating the design and operating variables for better debris removal efficiency almost always increases capital and operating cost.

In the 1950's and early 1960's, Bradley and a number of other investigators combined various centrifugal cleaner operating and design variables into a series of theoretical, semi-empirical, and empirical models which can be collectively referred to as Bradley models, because Bradley summarized them in a 1965 text, now considered a classic.³³ Bradley and the others usually modeled d_{50} efficiency,

defined as the diameter at which 50% of the debris would be removed, for experimental and theoretical convenience. Most of the models' developments were based on calculating drag force, centrifugal force, and residence time within the cleaner. Equation 9 shows a typical Bradley d_{50} model:

$$d_{50} = \frac{3(0.38)^n}{\alpha} \left[\frac{\eta D_c (1 - R_f)}{Q(\sigma - \rho)} \tan \frac{\theta}{2} \right]^{0.5} \frac{D_i}{D_c} \quad (\text{Equation 9})^{33}$$

where D_c is the cleaner primary diameter, D_i is the inlet diameter, $n = 0.8$, Q is the feed flow rate, R_f is the flow split ratio, $\alpha = 0.45$, η = absolute viscosity of the suspending fluid, ρ = fluid density, σ = particle density, and θ = included angle of the cone.

Bradley has shown that Equation 9, and a number of other investigator's d_{50} models can be reduced to the form shown in Equation 10:

$$d_{50} = a \left[\frac{D_c^3 \eta}{Q(\sigma - \rho)} \right]^{0.5} \quad (\text{Equation 10})$$

which assumes that $R_f = 0.1$, $\alpha = 0.45$, $n = 0.8$, and $\theta = 9^\circ$. When D_c is in cm, η is in cp, Q is in ℓ/min , $(\sigma - \rho)$ is in g/cm^3 , Bradley's value for a is 4.1, to yield d_{50} in μm . Bradley showed that the value for a is 1.8-14.6 for the similarly reduced form of other investigator's d_{50} models.³³

These models are typically accurate only for small diameter (7.6 cm primary diameter is typical), low flow rate (small inlet area) hydraulically smooth forward cleaners, operating on low consistency slurries of spherical particles. The latter condition is significant, because all of the models were developed for use in the mining and mineral dressing industry, where suspended particles do not interfere with the free migration of other particles. This is not the case in paper industry applications, where cellulose fibers have been shown to interfere with particle removal quite significantly. Thus, the Bradley type models are not useful for predicting absolute debris removal efficiency in practical paper industry applications, but they can be used for evaluating the relative effect of various operating parameters.³⁴

For example, Equations 9 and 10 can be used to predict the previously identified design and operating characteristic effects on debris removal efficiency (except for feed consistency, and surface characteristics). They can also be used to show that sand (density $>2.5 \text{ g}/\text{cm}^3$) will be removed with much greater efficiency than adhesives (density = 0.89-1.3 g/cm^3); and, that increasing temperature will improve

the removal of marginal debris much more than that of easily removed debris.³⁴

This point will be further demonstrated by using Equations 9 and 10 to explain an unexpected trend recently shown in the literature. A number of recent papers have shown quite clearly that hot melt adhesive (HMA) particles are difficult to remove with reverse and through flow cleaners when the density of the particle is close to 1.0 g/cm^3 . Wise, et.al.,⁸ and Bormett, et.al.³⁵ have shown that removal efficiency is greatly reduced when the density of the HMA is between 0.98 and 1.05 g/cm^3 . In addition, both groups also showed some evidence that smaller HMA particles are removed at lower efficiency than larger particles of the same density, given equal hardware and operating conditions. This work has resulted in the call for HMA producers to avoid marketing HMAs in the paper industry within the density range that has been identified as difficult to remove.³⁶

Unfortunately, many polymers can change their density when immersed in stock, due to leaching of certain components out of the adhesive, absorption of water, or surface adsorption of other components (ink, minerals, oil, etc.), and due to differential thermal expansion. For example, Table 6 lists typical water absorption values for various polymers.³⁷

The coefficient of linear thermal expansion for polymers varies over a range of about $4-20 \times 10^{-5}/^\circ\text{C}$, which brackets the thermal expansion of water. The linear thermal expansion coefficients for various polymers are also listed in Table 6.^{24,25,37}

Table 6: Water absorption and coefficient of linear thermal expansion for various polymers.

| Polymer | Water absorption (%) | Linear expansion coefficient, α ($\times 10^{-5}/^\circ\text{C}$) |
|----------------------------------|----------------------|--|
| Polyethylene | | 10-20 |
| Polypropylene | | 5.8-10 |
| Ethylene/vinyl acetate copolymer | 0.5-1 | 16-20 |
| Polyvinylacetate | 2.5-3 | 12-13 |
| Polyvinylchloride | 0.2-2.0 | 5-18 |
| Polystyrene | 0-0.2 | 4-7 |
| Styrene-butadiene rubber | 0.2-0.6 | 20-22 |
| Latex rubber | 1.0-2.0 | 20-21 |
| Waxes | | 100-125 |
| Nylon 6/6 | | 8.0 |

While Table 6 shows that some polymers absorb quite significant amounts of water, EVA, the major component of many HMA formulations, absorbs very little water. Further, absorption of a few weight percent of water will have almost no effect on the density of HMA particles that are already close to the density of water.

Adsorption of oils on the surface is the proposed mechanism of liquid bridge agglomeration,³⁸ and adsorption of (high density) minerals, especially talc, has been demonstrated to increase the apparent density of some pressure sensitive adhesives, as well as change their surface properties (i.e. reduce tackiness).³⁹ Adsorption of inks on sticky adhesives, and also on the surface of some film type plastics is clearly shown in many mills, by the black appearance of such materials.

Further, some adhesives are applied with air inadvertently included within the bulk of the material. Thus, even if the basic material density is well known and stable, the density of a given particle may be dramatically lower if an air bubble is included.

Overall, it is clear that the potential for deviation from the nominal density of the adhesive as listed by the manufacturer is quite significant. Unfortunately, most investigators to date have used the adhesive manufacturer's nominal density data, with no corrections applied, or measured the adhesive density only at room temperature, and in pure water, brine, oil, or something other than mill process water.

The debris removal efficiency of reverse cleaners improves dramatically with increasing temperature, as predicted by the viscosity term in Equations 9 and 10, and as reported in the literature.⁹ However, Maze⁴⁰ has recently published data that shows a slight decrease in the debris removal efficiency as the temperature increased, for adhesive particles of 0.995 g/cm³ specific gravity (the manufacturer's reported value). This unusual trend can be explained via Equations 9 and 10, by examining the effect of water absorption and increasing temperature on water viscosity, water density, and adhesive density.

Ignoring the effect of water absorption, since the nominal density is close to that of water, Equation 10 is rewritten substituting $(\rho - \sigma)$ for the density difference term, for use in describing a reverse cleaner. Pressure drop is taken as 275 kPa, and the Yoshioka and Hotta relationship is used to determine the feed flow rate for the cleaner, as shown in Equation 11:³³

$$dp = \frac{39Q^2}{D_c^4} \quad (\text{Equation 11})$$

where dp is the pressure drop, in psi; Q is the flow rate in ℓ/min , and D_c is the primary diameter, taken as 7.6 cm in this case. This results in a value for Q of 58.4 ℓ/min .

The rate of thermal expansion often varies with temperature; however, a reasonable approximation for volume expansion is given by Equation 12:²⁵

$$V_t = V_0(1 + \beta t) \quad (\text{Equation 12})$$

where V_t = volume at temperature = t , V_0 = volume at 0°C, β = volumetric expansion coefficient, and t = temperature, °C. A common approximation for $\beta = 3\alpha$.

Taking $\alpha = 4.1$ for Equation 10, using published values for the density of water from 20-60 °C, and assuming a density of 0.99 g/cm³ at 20 °C for this example, the value of d_{50} is calculated and plotted against temperature for $\beta = 12$ and $60 \times 10^{-5}/^\circ\text{C}$ (3 times the high and low values of α from Table 6). These results appear in Figure 9.

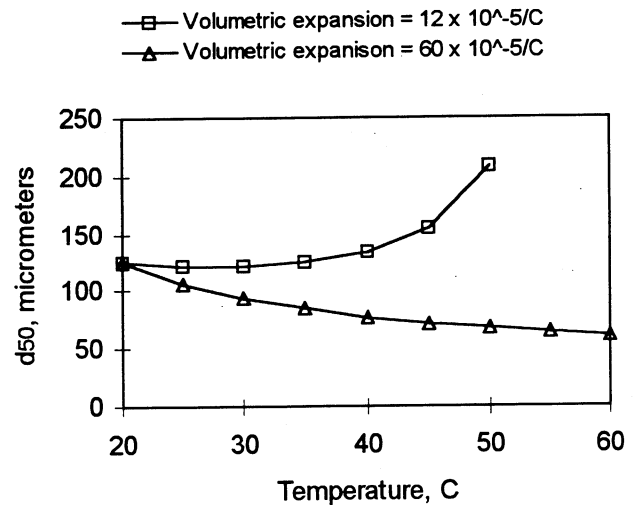


Figure 9: d_{50} vs. Temperature for adhesive particles with high and low thermal expansion characteristics.

Figure 9 shows that as temperature increases, the net effect of density changes for both the particles and the water, and the reduction in the water viscosity, results in a reduction in the d_{50} diameter when the thermal expansion coefficient is high. This indicates a shift towards higher debris removal efficiency, as predicted more generally with increasing temperature. If the thermal expansion coefficient is lower than that of water (which ranges from 20-52 $\times 10^{-5}/^\circ\text{C}$ within the indicated temperature range), the d_{50} diameter may actually increase. This would result in a debris removal efficiency decrease with increasing temperature, as reported

by Maze.⁴⁰ This is the case for the upper curve in Figure 9, which shows that d_{50} approaches infinity above 50 °C for the low thermal expansion case, because the debris particle density has become higher than that of the water.

The above example is important only when the particle density is close to that of water, which is an area of ongoing interest to applied researchers at the present moment. Again, it is clear that great care must be taken to determine the density of adhesives while they are at equilibrium with mill process water, and at the process temperature, especially when their density is close to that of the suspending liquid.

The Bradley models are thus shown to be useful for explaining normal debris removal efficiency trends, and also for explaining otherwise contradictory data in the literature.

Suspended Solids Washers

It is often necessary to remove both dissolved and suspended solids from recycled fiber slurries. By definition, dissolved solids are homogeneous at the molecular level, and hence are removed proportional to the removal of water during any dewatering operation, with minor exceptions for molecules bound via adsorption to the fiber surfaces, and for counterions. By comparison, suspended solids are by definition finite size particles which are not dispersed homogeneously at the molecular level, although those below 0.001 μm diameter may be considered to be colloidal, and may be expected to behave more or less as dissolved solids.

Suspended solids washing is capable of removing a variety of undesirable components, including ink, mineral particles, fiber fines, and very small adhesive particles. The efficiency of removal of each component is highly dependent on the characteristic particle size, the type of washing hardware, and the washer operating conditions. Table 7 lists the characteristic dimensions of some fine suspended solids components which may be candidates for removal via washing.

Table 7: Characteristic dimensions of fine suspended solids.

| Particle type | Size range (μm) | Shape |
|---------------------------------------|------------------------------|----------------------------|
| Fiber fines | <200 | fibrils, flakes, cubical |
| Clay (coating) | < 20 | plate-like |
| Clay (filler) | 0.5-10 | plate-like |
| TiO ₂ | 0.15 | spherical |
| CaCO ₃ | 0.5-3.0 | irregular/spherical |
| Talc | 0.5-5.0 | plate-like |
| Offset ink | 2-100 | small flakes, or ink balls |
| Toner flakes | 10-500 | thin flakes |
| Flexographic ink | 0.3-2.0 | spherical |
| Coating flakes | 10-500 | flake |
| Precipitated non-process elements, | any? | Spherical/cubical? |
| Precipitated or agglomerated adhesive | any? | Spherical/cubical? |

The historical view of suspended solids washing is that particles smaller than about 10 μm will follow the water split during washing, while progressively larger particles will be removed at progressively lower fractions of the water split. This tendency is shown in the now-classic illustration first proposed by Horacek in 1979,⁴¹ and widely reproduced since then, for removal of offset ink particles with screw presses. A version of this illustration, shown in Figure 10, plots washer discharge consistency against washer efficiency factor, which is the ratio of actual to theoretical washing efficiency. Washer efficiency factor could also be defined as the ratio of the percent of suspended solids removed, to the percent of water removed.

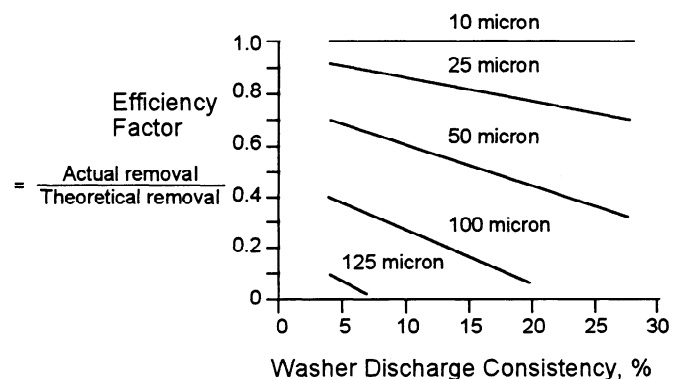


Figure 10: Washer discharge consistency vs. efficiency factor for screw presses (adapted from Horacek⁴¹).

Figure 10 alone does not explain why the larger particles are removed with lower efficiency, although the text reference clearly suggests that this is due to mechanical entrapment of the ink particles by the fiber mat. Today, we believe that a more complete explanation would require a discussion of filtration theory, washing chemistry, and mat characteristics.

Particles can be retained by a fiber mat by any of three mechanisms: mat surface capture, internal sieving, and fiber surface capture.⁴² Particles which are far too large to enter the spaces between the fibers in a fiber mat, accumulate as a filtercake, which then acts as the filtration media, on the face of the fiber mat. Smaller particles can enter the mat, and are mechanically captured by the internal restrictions within the mat, due to internal sieving. Very small particles, which could easily pass through the spaces between the fibers, are sometimes captured on the fiber surfaces by surface attraction forces. These three mechanisms are illustrated in Figure 11.

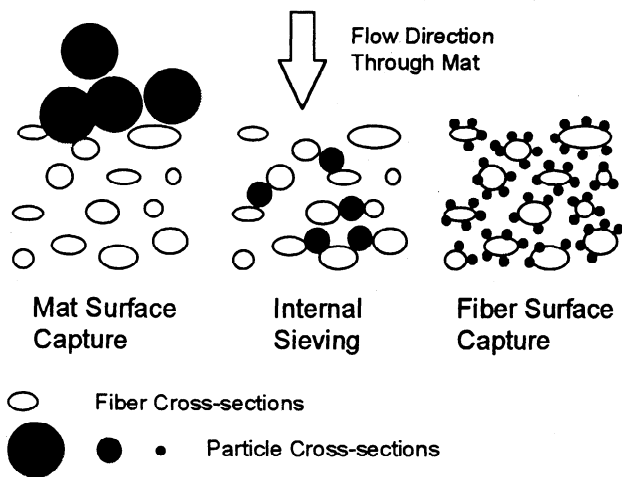


Figure 11: Particle capture mechanisms: mat surface capture, internal sieving, and fiber surface capture (adapted from Raistrick⁴²).

Fiber surface capture, based on surface attraction forces, is familiar to the papermaker as the primary mechanism of filler retention at the wet end of the paper machine. Such retention is applicable only to particles below 1-5 μm , because larger particles have too little contact area to be held in place by these weak forces as liquid moves across the particles, creating drag force. In other words, higher shear conditions reduce the retention of small particles, or increase their efficiency of removal during washing.

Surface attraction forces are also very sensitive to surface chemistry conditions; a knowledge of the surface charge

response of the fine particles to pH is important. Cellulose fibers carry a negative surface charge, which becomes more negative as pH increases. At low pH, most fillers carry a positive surface charge, while at high pH, most fillers carry a negative charge. Thus, in the absence of a retention aid, most minerals are more effectively washed out at the higher pH's found in deinking systems than at low or neutral pH, because the opposite-charge attraction force is neutralized, or even replaced with a same-charge repulsive force.

By comparison, polymeric particles in general can carry a positive, neutral, or negative charge, depending on the number and type of groups on the polymer chain, and depending on the pH.

The retention tendencies of non-soluble organic particles, including oil-based inks, are also affected by micelle formation. Since most inks and polymers are hydrophobic, they readily attract the hydrophobic end of surfactant molecules, while allowing the hydrophilic end of each surfactant molecule to interact with the water molecules in the bulk of the suspension. This structure, called a micelle, is illustrated in Figure 12. Micelle structures allow otherwise insoluble dirt particles in suspensions to remain independent of association with the fiber surfaces, except for the potential for mechanical entrapment via internal sieving or mat surface capture.

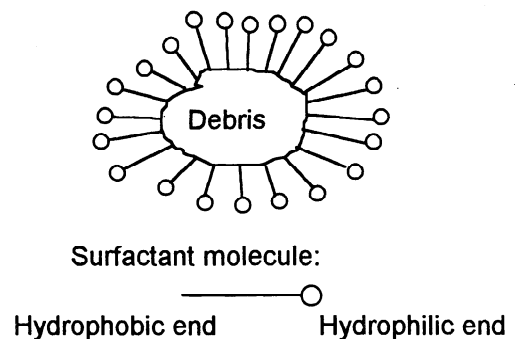


Figure 12: Popular depiction of a surfactant micelle. The surfactant molecules are grossly oversize relative to the suspended solids particle, to illustrate the structure.

Mat characteristics and integrity mechanically control particle capture by internal sieving and mat surface capture, assuming they are not bound to the fiber surface due to pH and surface chemistry. Since the clearance between fibers within the mat is a function of both mat consistency and fiber coarseness, fiber type as well as mat consistency are believed to be important. The importance of fiber coarseness, mat density (consistency), and fiber orientation within the mat is the subject of our current research, and will be reported at a future date.

The importance of mat integrity can be clearly seen by comparing the turbulence level, hydraulic split range, and washing effectiveness of commercial washers. Figure 13 ranks the major classes of commercial washers by turbulence level, hydraulic split range, and inlet/outlet consistency.⁴³ The range of solids losses for the various types of washers, as listed in Table 8, can be compared with these characteristics.

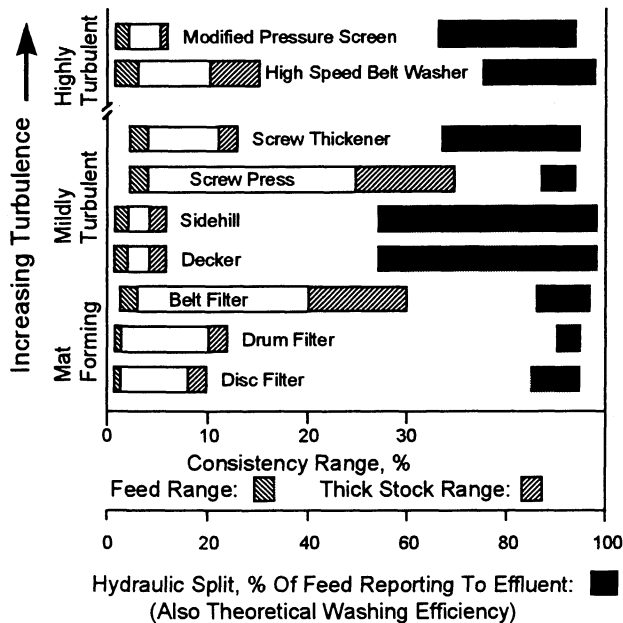


Figure 13: Characteristics of commonly used commercial washing devices

Table 8: Typical suspended solids loss range of commonly used commercial washers on 70% news/30% magazine furnish.

| Washer type | Solids loss range (% of feed) |
|---|-------------------------------|
| Mat Forming: (Disc, drum, and belt filters) | 1-5 |
| Mildly Turbulent: (Deckers, sidehill screens, screw presses, and screw thickeners) | 10-25 |
| Highly Turbulent: (High speed belt washers, and modified pressure screens) | 25-45 |

As shown in Figure 13 and Table 8, the low shear, mat-forming washers have a very high hydraulic split range, and a very low suspended solids loss range. This suggests that

they are not effective for removal of suspended solids, although the suspended solids removed are generally free of fiber. It would be fair to say that low speed mat forming washers are better thickeners and dissolved solids washers than suspended solids washers.

By comparison, the mildly turbulent washers are characterized by a wide hydraulic split range (except for the screw press), less mat integrity, and higher suspended solids losses. They are better suspended solids washers, but the larger screen plate openings typically found in these devices, and the higher level of turbulence (poor mat integrity) also allow considerably higher amounts of fiber to be lost.

The highly turbulent washers operate in a very high shear environment, and mat integrity is almost nil. They are excellent suspended solids washers, but they also allow the highest suspended solids losses. As with most of the other washers, the loss of useable fiber is highly dependent on the operating conditions and the media opening size.

CONCLUSIONS

Debris properties can profoundly affect removal efficiency with common debris removal devices in fiber recovery systems. In particular:

- 1) Debris particle size broadly determines the type of device best suited for removal of the particle. Particle size is also one of many factors which determines the effectiveness of a given device. Adhesives, a particularly troublesome class of debris, are often reduced in size to the range where they must be removed via pressure screens, centrifugal cleaners, froth flotation, and washing.
- 2) Debris particle size and shape can dramatically affect removal efficiency in pressure screens. Debris particles with 1-long and 2-long dimensions can be accepted or rejected based on alignment. Particle shape ratio may affect removal efficiency, even for particles which are only slightly non-spherical, relative to normal dimension ratio requirements for hydraulically induced orientation.
- 3) Particle mechanical properties, such as stiffness and yield stress, may be critical for acceptance or rejection of soft adhesive particles, according to proposed bending and extrusion mechanisms.
- 4) In addition to particle size, the difference in density between the debris particle and the suspending liquid is quite critical in centrifugal cleaners. This difference cannot be assumed to be constant due to the potential for particles to leach, swell, absorb water, or adsorb oils or minerals. Great care must be taken in analyzing particle

removal efficiency data when the particle density is close to the density of water.

- 5) Particle shape and density probably play a lesser role for suspended solids washing. Instead, surface chemistry, and mat characteristics, such as fiber coarseness, mat density, and degree of mat integrity or shear, are more important.
- 6) Further research is needed to better understand the complex interrelationships between debris particle properties and mechanisms of debris removal in commonly utilized debris removal devices.

REFERENCES

1. McCool, M. A., and Silveri, L., "Removal of Specks and Non-dispersed Ink from a Deinking Furnish," *Tappi Journal* 70(11):75-79 (1987).
2. Moss, C. S., "Theory and Reality for Contaminant Removal Curves," *Tappi Journal* 80(4):69-74 (1997).
3. Bliss, T., "Screening," Ch. 14 from *Secondary Fiber Recycling*, (R. J. Spangenberg, ed.), 1st ed., TAPPI PRESS, Atlanta, GA (1993).
4. Whiting, P.L., "Contaminant Control on a High Speed Paper Machine," Proceedings, 1996 Tappi Pulping Conference, TAPPI PRESS, Atlanta, GA, 285-289 (1996).
5. Friberg, T., "Cost Impact of Stickies," *Progress in Paper Recycling* 6(1): 70-72 (1996).
6. Douek, M., "Overview of Research on Stickies at Pulp and Paper Research Institute of Canada (PAPRICAN)," from *Paper Recycling Challenge*, 1st ed., Vol. 1 *Stickies*, (M. R. Doshi and J. Dyer, eds.), Doshi & Associates, Inc., Appleton, WI, 15-21. (1997).
7. Doshi, M. "Properties and Control of Stickies," from *Paper Recycling Challenge*, 1st ed., Vol. 1 *Stickies*, (M. R. Doshi and J. Dyer, eds.), Doshi & Associates, Inc., Appleton, WI, 227-235. (1997).
8. Wise, E. M., and Arnold, J. M., "The Role of Specific Gravity for the Removal of Hot Melt Adhesives in Recyclable Grades," *Tappi Journal* 75(9): 181-185 (1992).
9. Bliss, T., "Reverse Cleaning Its Use in Removing Lightweight and Sticky Contaminants," *Tappi Journal* 63(6): 87-90 (1980).
10. Stratton, R. A., "The Flotation of Sticky Contaminants from Recycled Streams," *Progress in Paper Recycling* 1(4):31-37 (1992).
11. Ling, T. F., "The Effects of Surface Properties on Stickies Removal by Flotation," *Pulp & Paper Canada* 95(12): 109-113 (1994).
12. Horacek, R. G., "Washing Ink from the Pulp Slurry," Ch. 17 from Vol. 3, *Secondary Fiber and Nonwood Pulping*, (F. Hamilton and B. Leopold, volume eds.), Pulp and Paper Manufacturing Series, Joint Textbook Committee of the Paper Industry, 189-205 (1987).
13. Fetterly, N., "The Role of Dispersion Within a Deinking System," *Progress in Paper Recycling* 1(3): 11-20 (1992).
14. (Various authors), *Handbook of Adhesives*, 3rd ed., (I. Skeist, ed.), Van Nostrand Reinhold, New York, NY (1990).
15. (Various authors), *Handbook of Pressure Sensitive Adhesives*, 1st ed., (D. Satas, ed.), Van Nostrand Reinhold, New York, NY (1982).
16. Hsu, N. N-C., "Stickies The Importance of Their Chemical and Physical Properties," from *Paper Recycling Challenge*, 1st ed., Vol. 1 *Stickies*, (M. R. Doshi and J. Dyer, eds.), Doshi & Associates, Inc., Appleton, WI, 256-258 (1997).
17. Yu, C. J., Crossley, B. R., and Silveri, L., "Fundamental Studies of Screening Hydraulics Part 3: Models for Calculating Effective Open Area," *Tappi Journal* 77(9): 125-131 (1994).
18. Yu, C. J., and Defoe, R., "Fundamental Studies of Screening Hydraulics Part 2: Fiber Orientation on the Feed Side of the Screen Basket," *Tappi Journal* 77(9): 119-124 (1994).
19. Gooding, R. W., and Kerekes, R. J., "The Motion of Fibres Near a Screen Slot," *Journal of Pulp and Paper Science* 15(2): J59-62 (1989).
20. Bliss, T., and Vitori, C., "Effect of Velocity Through Pressure Screen Slots on Efficiency and Throughput," Proceedings, 1992 Tappi Contaminant Problems & Strategies in Waste Paper Seminar, TAPPI PRESS, Atlanta, GA, 73-84

- (1992).
21. Vitori, C. M., "Stock Velocity and Stickies Removal Efficiency in Slotted Pressure Screens," Proceedings, 1st Research Forum on Recycling, Technical Section, CPPA, Montreal, CANADA, 133-142 (1991).
 22. Pikulin, M. A., "Stickies and Their Impact on Recycled Fiber Content Fine Papers," from *Paper Recycling Challenge*, 1st ed., Vol. 1 *Stickies*, (M. R. Doshi and J. Dyer, eds.), Doshi & Associates, Inc., Appleton, WI, 89-93 (1997).
 23. Heise, O., "Screening Foreign Material and Stickies," *Tappi Journal* 75(2): 78-81 (1992).
 24. Gere, J. M., and Timoshenko, S. P., *Mechanics of Materials*, 3rd ed., PWS Publishing Co., Boston, MA (1990).
 25. Weast, R. C. (ed.), *Handbook of Chemistry and Physics*, 56th ed., CRC Press, Cleveland, OH (1975).
 26. Steiner, T., Personal communication, 3M Company, St. Paul, MN, June 1997.
 27. (Unattributed), "Adhesives," from *Encyclopedia of Chemical Technology*, 4th ed., Vol. 1, John Wiley & Sons, 453 (1991).
 28. Zyczkowski, M., *Combined Loadings in the Theory of Plasticity*, Polish Scientific Publishing, Warsaw, Poland (1981).
 29. Naddeo, R. C., Hristofus, K., and Magnotta, V. L., US Patent No. 5,213,661 (May 25, 1993).
 30. Naddeo, R. C., Hristofus, K., and Magnotta, V. L., US Patent No. 5,338,401 (Aug. 16, 1994).
 31. Naddeo, R. C., Magnotta, V. L., Kulikowski, T., Ayala, V., and Jezerc, G., "Oxidative Methods Offer Alternative to Chlorine Bleaching of Wastepaper," *Pulp & Paper* 66(11): 71-74, 78, 80-81 (1992).
 32. Bliss, T., "Centrifugal Cleaning" Ch. 13 from Volume 6, *Stock Preparation and Wet End Additives*, 3rd ed., (R. W. Hagenmeyer and M. J. Kocurek, volume eds.), Pulp and Paper Manufacturing Series, Joint Textbook Committee of the Paper Industry, 248-261 (1992).
 33. Bradley, D., *The Hydrocyclone*, Pergamon Press, New York, NY (1965).
 34. Bliss, T., *Stock Cleaning Technology*, Pira International, Surry, UK (1997).
 35. Bormett, D. W., Lebow, P. K., Ross, N. J., and Klungness, J. H., "Removal of Hot Melt Adhesives with Through-flow Cleaners," Proceedings, 1995 Tappi Polymers, Laminations, and Coatings Conference, TAPPI PRESS, Atlanta, GA, 257-262 (1995).
 36. Paper and Paperboard Packaging Environmental Council (of Canada), *PPEC News* 5(1): 3 (1995).
 37. Shields, J., *Adhesives Handbook*, 3rd ed., Butterworths, London, UK, 163-168 (1984).
 38. Snyder, B. A., and Berg, J. C., "Liquid Bridge Agglomeration: A Fundamental Approach to Toner Removal," *Tappi Journal* 77(5): 79-84 (1994).
 39. Yordan, J. L., and Williams, G. R., "Talc for Contaminant Control in Recycled Paper," from *Paper Recycling Challenge*, 1st ed., Vol. 1 *Stickies*, (M. R. Doshi and J. Dyer, eds.), Doshi & Associates, Inc., Appleton, WI, 76-80 (1997).
 40. Maze, E., "New Cleaner Development for Lightweight Contaminant Removal," *Progress in Paper Recycling* 6(3): 40-47 (1997).
 41. Horacek, R. G., *Beloit Corporation Deinking Manual*, Beloit Jones, Dalton, MA (1979).
 42. Raistrick, J. H., "The Relevance of Zeta Potential to Filtration and Separation of Small Particles from Potable Liquids," *Filtration Separation Science* 20(2): 124-126 (1983).
 43. Bliss, T., Seifert, P., and Dietrich-V, G., "Controlling Yield in Washing Deink Systems," Proceedings, 1994 Tappi Pulping Conference, TAPPI PRESS, Atlanta, GA, 1011-1024 (1994).
- Prepared for: 1997 Tappi Korea Recycling Symposium, October 16-17, 1997, Seoul, Korea
- Filename: debristext1.doc Terry Bliss 07/30/97 11:17 AM

